

*Soil and water assessment tool-based prediction of runoff under scenarios of land use/land cover and climate change across Indian agro-climatic zones: implications for sustainable development goals*

Article

Published Version

Creative Commons: Attribution 4.0 (CC-BY)

Open Access

Subbarayan, S. ORCID: <https://orcid.org/0000-0003-4085-1195>, Youssef, Y. M. ORCID: <https://orcid.org/0000-0001-5939-732X>, Singh, L. ORCID: <https://orcid.org/0000-0002-0734-4004>, Dąbrowska, D. ORCID: <https://orcid.org/0000-0002-6762-8885>, Alarifi, N. ORCID: <https://orcid.org/0000-0001-7802-5070>, Ramsankaran, R. ORCID: <https://orcid.org/0000-0001-8602-1934>, Visweshwaran, R. and Saqr, A. M. ORCID: <https://orcid.org/0000-0002-3458-1208> (2025) Soil and water assessment tool-based prediction of runoff under scenarios of land use/land cover and climate change across Indian agro-climatic zones: implications for sustainable development goals. *Water*, 17 (3). 458. ISSN 2073-4441 doi: <https://doi.org/10.3390/w17030458> Available at <https://centaur.reading.ac.uk/120932/>

work. See [Guidance on citing](#).

To link to this article DOI: <http://dx.doi.org/10.3390/w17030458>

Publisher: MDPI AG

All outputs in CentAUR are protected by Intellectual Property Rights law, including copyright law. Copyright and IPR is retained by the creators or other copyright holders. Terms and conditions for use of this material are defined in the [End User Agreement](#).

[www.reading.ac.uk/centaur](http://www.reading.ac.uk/centaur)









## **CentAUR**

Central Archive at the University of Reading

Reading's research outputs online

## Article

# Soil and Water Assessment Tool-Based Prediction of Runoff Under Scenarios of Land Use/Land Cover and Climate Change Across Indian Agro-Climatic Zones: Implications for Sustainable Development Goals

Saravanan Subbarayan <sup>1</sup>, Youssef M. Youssef <sup>2,\*</sup>, Leelambar Singh <sup>3</sup>, Dominika Dąbrowska <sup>4,\*</sup>, Nassir Alarifi <sup>5</sup>, RAAJ Ramsankaran <sup>6</sup>, R. Visweshwaran <sup>7</sup> and Ahmed M. Saqr <sup>8</sup>

- <sup>1</sup> Department of Civil Engineering, National Institute of Technology, Tiruchirappalli 620015, India; ssaravanan@nitt.edu
  - <sup>2</sup> Geological and Geophysical Engineering Department, Faculty of Petroleum and Mining Engineering, Suez University, Suez 43518, Egypt
  - <sup>3</sup> Department of Civil Engineering, Malaviya National Institute of Technology, Jaipur 302017, India; leelambar.ce@mnit.ac.in
  - <sup>4</sup> Faculty of Natural Sciences, University of Silesia, Będzińska 60, 41-200 Sosnowiec, Poland
  - <sup>5</sup> Department of Geology & Geophysics, College of Science, King Saud University, P.O. Box 2455, Riyadh 11451, Saudi Arabia; nalarifi@ksu.edu.sa
  - <sup>6</sup> Department of Civil Engineering, Indian Institute of Technology Bombay Powai, Mumbai 400076, India; ramsankaran@civil.iitb.ac.in
  - <sup>7</sup> Department of Meteorology, University of Reading, Berkshire RG6 6AH, UK; v.ramesh@reading.ac.uk
  - <sup>8</sup> Irrigation and Hydraulics Department, Faculty of Engineering, Mansoura University, Mansoura 35516, Egypt; ahmedsaqr@mans.edu.eg
- \* Correspondence: youssef.ibrahim@pme.suezuni.edu.eg (Y.M.Y.); dominika.dabrowska@us.edu.pl (D.D.)



Academic Editor: Richard Smardon

Received: 17 December 2024

Revised: 24 January 2025

Accepted: 25 January 2025

Published: 6 February 2025

**Citation:** Subbarayan, S.; Youssef, Y.M.; Singh, L.; Dąbrowska, D.; Alarifi, N.; Ramsankaran, R.; Visweshwaran, R.; Saqr, A.M. Soil and Water Assessment Tool-Based Prediction of Runoff Under Scenarios of Land Use/Land Cover and Climate Change Across Indian Agro-Climatic Zones: Implications for Sustainable Development Goals. *Water* **2025**, *17*, 458. <https://doi.org/10.3390/w17030458>

**Copyright:** © 2025 by the authors. Licensee MDPI, Basel, Switzerland. This article is an open access article distributed under the terms and conditions of the Creative Commons Attribution (CC BY) license (<https://creativecommons.org/licenses/by/4.0/>).

**Abstract:** Assessing runoff under changing land use/land cover (LULC) and climatic conditions is crucial for achieving effective and sustainable water resource management on a global scale. In this study, the focus was on runoff predictions across three diverse Indian watersheds—Wunna, Bharathapuzha, and Mahanadi—spanning distinct agro-climatic zones to capture varying climatic and hydrological complexities. The soil and water assessment (SWAT) tool was used to simulate future runoff influenced by LULC and climate change and to explore the related sustainability implications, including related challenges and proposing countermeasures through a sustainable action plan (SAP). The methodology integrated high-resolution satellite imagery, the cellular automata (CA)–Markov model for projecting LULC changes, and downscaled climate data under representative concentration pathways (RCPs) 4.5 and 8.5, representing moderate and extreme climate scenarios, respectively. SWAT model calibration and validation demonstrated reliable predictive accuracy, with the coefficient of determination values ( $R^2$ ) > 0.50 confirming the reliability of the SWAT model in simulating hydrological processes. The results indicated significant increases in surface runoff due to urbanization, reaching >1000 mm, 600 mm, and 400 mm in southern Bharathapuzha, southeastern Wunna, and northwestern Mahanadi, respectively, especially by 2040 under RCP 8.5. These findings indicate that water quality, agricultural productivity, and urban infrastructure may be threatened. The proposed SAP includes nature-based solutions, like wetland restoration, and climate-resilient strategies to mitigate adverse effects and partially achieve sustainable development goals (SDGs) related to clean water and climate action. This research provides a robust framework for sustainable watershed management in similar regions worldwide.

**Keywords:** SWAT; CA–Markov; land use/land cover; climate change; agro-climate; India; sustainable development goals

## 1. Introduction

Understanding and predicting runoff is vital for sustainable water resource management, especially in regions facing complex challenges due to rapid land use/land cover (LULC) changes and climate fluctuations [1]. Moreover, runoff can significantly influence soil erosion, water quality, and flood risk owing to alterations in LULC such as urbanization expansion, and climatic conditions, including rainfall intensity and seasonal variability [2]. Furthermore, the transformation of natural landscapes causes substantial changes to the hydrological cycle, resulting in increased frequency and severity of floods, erosion, and sedimentation [3]. These variables can exacerbate hydrological issues, particularly in regions undergoing substantial growth and climate-induced stresses, leading to severe environmental degradation [4]. Precisely forecasting runoff in these conditions is crucial for the implementation of adaptive management strategies aligned with the sustainable development goals (SDGs) [5]. In turn, reliable runoff prediction tools require trustworthy methods, adapted to various agro-climatic and socio-environmental conditions [6].

Diverse techniques have been utilized to forecast runoff, including statistical methods and process-based hydrological models [7]. While they are proficient in identifying correlations between rainfall, LULC, and runoff, statistical methods often inadequately represent the complexities of watershed hydrology due to a lack of focus on physical processes [8]. Process-based hydrological models incorporate LULC, soil properties, topography, and climatic factors to simulate complex hydrological responses, allowing them to better evaluate changes in runoff under varying environmental conditions [9]. The soil and water assessment tool (SWAT) has become prominent due to its adaptability and power in modeling hydrological processes in many environmental contexts [10]. It was developed by the Agricultural Research Service in the United States of America to evaluate runoff, sediment transport, and water quality, providing critical insights into the effects of climate change and LULC on watershed hydrology [11]. Multiple studies have confirmed the efficacy of SWAT, demonstrating its applicability in areas with changing LULC and climatic patterns [12]. In the Parvara Mula basin, India, SWAT was used to evaluate the impacts of climate change and LULC changes on streamflow under various climate change scenarios, revealing significant future increases in streamflow and aiding in the development of water management strategies [13]. Similarly, in the Nandu River basin on Hainan Island, China, SWAT was coupled with Markov modeling to analyze the effects of climate and LULC changes on hydrological processes, highlighting the dominant role of climate variables such as precipitation and temperature in influencing streamflow [14]. Additionally, a bibliometric analysis of SWAT applications in ecosystem services demonstrated its expanding use in quantifying water-related processes, soil retention, and ecosystem service flows, underscoring its value in holistic environmental and water resource management [15]. Despite its broad applications, it is essential to extend SWAT modeling to areas with diverse agro-climatic conditions and distinct LULC patterns to improve predictive accuracy and inform region-specific water management policies [16].

Globally, agro-climatic zones have significant challenges with runoff, especially as climate change intensifies precipitation patterns and human activity alters natural environments [17]. Regions like the Loess Plateau in China, the Alps in Europe, and the Amazon Basin in South America face distinct runoff-related issues, intensified by their particular climatic and LULC attributes [18]. These challenges are especially evident in India, where agro-climatic zones exhibit significant variation, encompassing desert, semi-arid, humid, and sub-humid regions [19]. The Indian Council of Agricultural Research (ICAR) categorizes the nation into the following 15 agro-climatic zones: Island Region, Western Dry Region, Gujarat Plains and Hills, West Coast Plains and Hills, East Coast Plains and Hills, Southern Plateau and Hills, Western Plateau and Hills, Central Plateau and Hills,



Eastern Plateau and Hills, Trans-Gangetic Plains, Upper Gangetic Plains, Middle Gangetic Plains, Lower Gangetic Plains, Eastern Himalayan, and Western Himalayan [20]. Each region has distinct runoff-related issues, ranging from soil erosion in elevated landscapes to waterlogging and inundation in low-lying agricultural areas [21]. In India, where water resources are crucial for agricultural and rural lives, forecasting runoff under changing LULC and climatic conditions is critical for sustainable management [22].

Despite growing concerns, there are few comprehensive runoff prediction studies tailored to India's diverse agro-climatic zones. In this study, we seek to address this significant research gap in runoff prediction research by adopting the SWAT model to investigate the Wunna, Bharathapuzha, and Mahanadi watersheds, in Western Plateau and Hills, West Coast Plains and Ghats, and Eastern Plateau and Hills Indian agro-climatic regions. These three watersheds were specifically selected to represent the diversity of agro-climatic zones in India, reflecting distinct variations in hydrological, climatic, and LULC characteristics, which make them ideal for assessing the impacts of LULC and climate changes on runoff dynamics. Additionally, in this study, the first evaluation is presented of the SDG-related implications of the anticipated runoff in agro-climatic regions. Hence, the study objectives are as follows: (a) utilizing the SWAT model to forecast runoff characteristics in the Wunna, Bharathapuzha, and Mahanadi watersheds under integrated climate change and LULC scenarios, (b) identifying sustainability challenges induced by the anticipated runoff in the three watersheds, and (c) proposing a sustainable action plan (SAP), which explicitly links innovative strategies to specific environmental, economic, and social SDG targets in order to mitigate any harmful consequences of the predicted runoff. In this research, a framework is provided for sustainable water management with applicable insights for similar watersheds encountering analogous LULC and climate-induced hydrological issues worldwide.

## 2. Materials and Methods

### 2.1. Watersheds Under Investigation

Three unique watersheds from diverse agro-climatic regions in India were selected to encompass a wide range of hydrological and environmental conditions (Figure 1a). Each watershed is located in a distinct geographical and climatic context, exemplifying the diversity of India's river basins, LULC, and precipitation patterns. The Wunna watershed represents a semi-arid, sub-humid area characterized by basaltic geology, rendering it important for the examination of runoff in agricultural environments. The Bharathapuzha watershed, situated in the humid tropical zone of the Western Ghats, is essential for evaluating runoff effects in regions characterized by significant rainfall and steep gradients. The Mahanadi watershed, located in the eastern plateau, exemplifies sub-humid climates characterized by a combination of agricultural and woodland areas, offering insights into runoff in regions affected by varied land-use patterns. The following paragraphs provide a detailed description of each selected watershed.

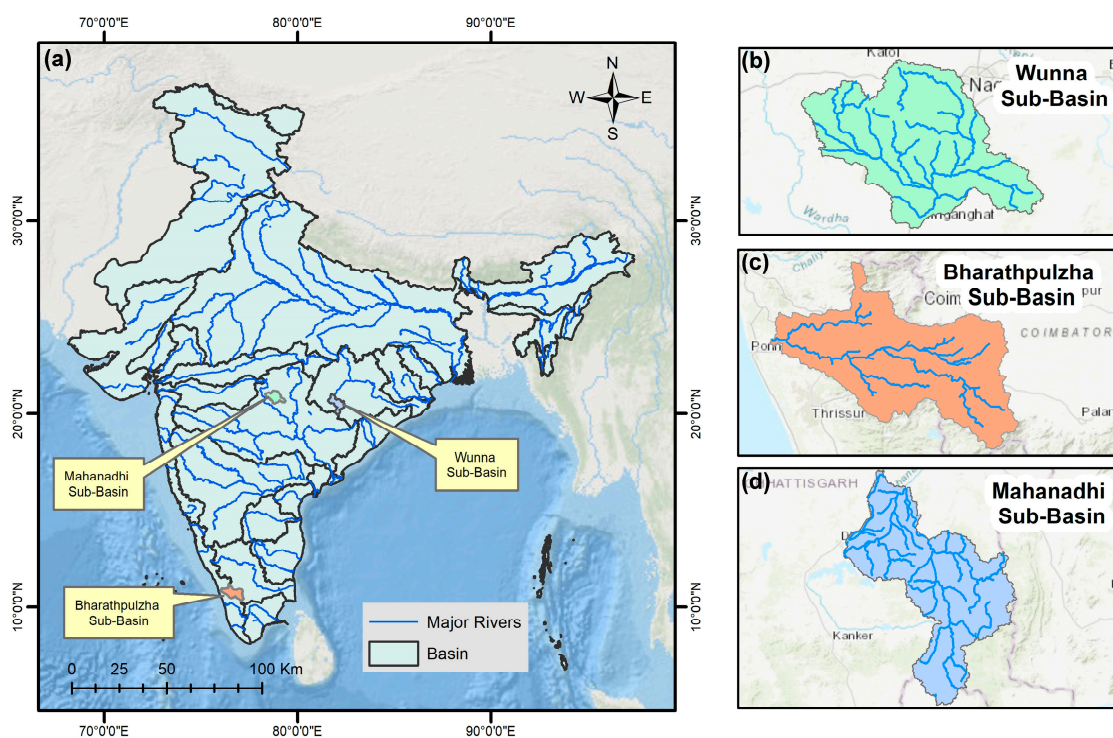


**Figure 1.** A map showing the location of the Indian agro-climatic watersheds under investigation: (a) The major river basins of India, highlighting the Wunna, Bharathapuzha, and Mahanadi sub-basins; (b) Wunna Sub-Basin; (c) Bharathapuzha Sub-Basin; and (d) Mahanadi Sub-Basin.

#### 2.1.1. Wunna Watershed

The Wunna watershed falls within Agro-Climatic Zone 6: The Central Plateau and Hills Region. It constitutes a minor segment of the Wardha sub-basin within the Godavari River basin. The Wunna River traverses from the Nagpur district to the Wardha district in Maharashtra, receiving most of its precipitation during the monsoon season from June to September. Geographically, it is situated between latitudes  $20^{\circ}28'$  and  $21^{\circ}15'$  N and longitudes  $78^{\circ}19'$  and  $79^{\circ}06'$  E, covering an area of  $4512 \text{ km}^2$  (Figure 1b). This watershed has an elevation range between 169 and 610 m, with an annual average precipitation of 1281 mm. The average maximum and minimum temperatures of the watershed are  $47.5^{\circ}\text{C}$  and  $15.2^{\circ}\text{C}$ , respectively. With over 60% of the land designated for agriculture, the utility of the watershed is high. The Nandgaon discharge gauge station has been used to delineate the watershed. The Wunna watershed is classified as a sub-humid and is primarily underlain by basalt, with red and black soils [23].

#### 2.1.2. Bharathapuzha Watershed

The Bharathapuzha watershed is located within Agro-Climatic Zone 12: The West Coast Plains and Ghats Region. It is positioned between the states of Kerala and Tamil Nadu, geographically situated between latitudes  $10^{\circ}25'$  and  $11^{\circ}15'$  N and longitudes  $75^{\circ}50'$  and  $76^{\circ}55'$  E (Figure 1c). It encompasses an area of  $5789.49 \text{ km}^2$ , with an elevation range between 3 and 2493 m, reflecting the steep gradients of the Western Ghats. This region receives much of its precipitation from the Indian monsoon, averaging 2340 mm annually. The Bharathapuzha River originates in the Anaimalai Hills of the Western Ghats and empties into the Arabian Sea near Ponnani. Average temperatures range from  $19.2^{\circ}\text{C}$  to  $32.4^{\circ}\text{C}$ . The Kumbidi discharge gauge station serves as a reference point for delineating the watershed. The Bharathapuzha watershed is classified as a hot-humid region, characterized by red, lateritic, and alluvial soils, underlain predominantly by gneiss and charnockite formations [24].

### 2.1.3. Mahanadi Watershed

The Mahanadi watershed is located in Chhattisgarh and lies between latitudes 20°0' and 21°05' N and longitudes 81°10' and 83°01' E, forming part of the middle Mahanadi sub-basin (Figure 1d). It covers 4533 km<sup>2</sup> and has an elevation range between 242 and 971 m. It primarily receives rainfall during the monsoon season, totaling an average of 1508 mm annually. The Mahanadi River originates in the Sihawa mountain range, and the watershed experiences temperature variations between 13.2 °C and 41.1 °C. The Rajim discharge gauge station has been proposed as an outlet point for delineation. The Mahanadi watershed is classified as a sub-humid, containing black and yellow soils, with geological formations including the banded Gneissic complex, sandstone, shale, and limestone aquifers [25].

### 2.2. Research Methodology

The methodology employed in this study integrated several advanced approaches that might outperform other geographic information systems (GIS)-based tools, such as public participation GIS (PPGIS), community mapping, and multi-scale geographically weighted regression (MGWR), in the context of hydrological modeling and LULC predictions. While tools like PPGIS and community mapping excel in participatory decision-making and incorporating stakeholder perspectives, and MGWR is effective for exploring spatial relationships across scales, they are less suited for capturing the dynamic interactions between land-use changes, climate variability, and hydrological processes over time [26]. By combining the SWAT with cellular automata (CA)-Markov modeling, high-resolution satellite imagery, and representative concentration pathway (RCP)-based climate projections, the methodology adopted in this study provided a robust and precise framework for assessing runoff patterns. In addition, it can offer a comprehensive approach to understanding and addressing the challenges of water resource management in diverse watersheds.

The SWAT model, chosen for its versatility and robust application in hydrological studies, has been extensively used to model runoff, assess the impacts of climate and land-use changes, and support water resource management under diverse environmental and agro-climatic conditions. Previous studies have validated SWAT's capability for simulating hydrological processes with high accuracy, making it a reliable choice for this research [27]. To project future LULC changes, the CA-Markov model was employed, a technique widely recognized for its ability to simulate LULC dynamics by combining the predictive power of CA with the stochastic properties of Markov chains. This model has been applied successfully in studies focused on predicting LULC transitions under various scenarios, further demonstrating its feasibility for capturing spatial and temporal changes [28]. High-resolution satellite imagery and climate datasets, including projections based on RCP 4.5 and RCP 8.5 scenarios, were integrated to ensure accurate representation of baseline conditions and future changes [29]. These climate scenarios allowed for the evaluation of runoff patterns under moderate and high conditions, aligning with global climate modeling standards. The incorporation of these methodologies allowed for a comprehensive analysis of the geologic, hydrologic, and land-use characteristics of the Wunna, Bharathapuzha, and Mahanadi watersheds, ensuring the robustness of the findings. The research framework adopted in this study was supported by a wealth of studies in the prior literature, demonstrating the effectiveness of integrating SWAT, CA-Markov, and advanced datasets for similar hydrological and environmental assessments [30]. The overall workflow and its components are summarized in Figure 2, illustrating the stepwise approach employed in this study.

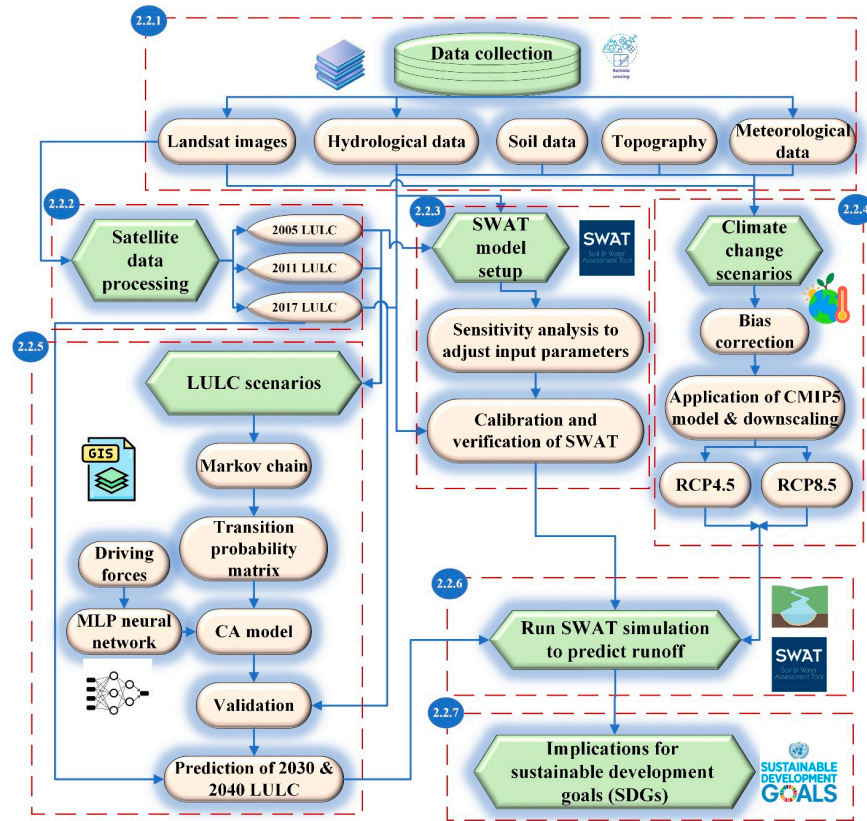


**Figure 2.** A flowchart describing the steps in the methodology.

2.2.1. Data Collection

Different types of data were collected to construct the SWAT model effectively. These data types include topography, soil, climate, and hydrological information, summarized as follows:

- Landsat images

Three distinct sets of Landsat satellite bands for the years 2005, 2011, and 2017 were obtained from the United States Geological Survey (USGS) website [31]. The characteristics of the satellite images utilized in this study are detailed in Table 1, including the acquisition dates, satellite/sensor types, and coordinate system specifications for the Mahanadi, Wunna, and Bharathapuzha watersheds.

**Table 1.** Characteristics of the satellite images utilized in this study.

Watershed	Acquired Date	Satellite/Sensor	Collection/Level	Coordinate System/Datum	Zone
Mahanadhi	22 December 2017	Landsat 08/TM	Collection 1/Level-1	UTM/WGS84	44
	4 November 2011	Landsat 05/TM			
	19 November 2005	Landsat 05/TM			
Wunna	20 October 2017	Landsat 05/TM	Collection 1/Level-1	UTM/WGS84	44
	24 October 2011	Landsat 07/ETM+			
	4 September 2005	Landsat 05/TM			
Bharathapuzha	8 January 2017	Landsat 08/OLI	Collection 1/Level-1	UTM/WGS84	43
	8 February 2011	Landsat 07/ETM+			
	16 October 2005	Landsat 05/TM			

Notes: TM = thematic mapper; ETM+ = Enhanced Thematic Mapper Plus; OLI = Operational Land Imager; UTM = Universal Transverse Mercator; and WGS84 = World Geodetic System 1984.



- Topography

The watershed's topography was developed using the Advanced Spaceborne Thermal Emission and Reflection Radiometer (ASTER) global digital elevation model (DEM) with a 30 m resolution, sourced from the Earth data web portal [32].

- Soil data

The global digital soil map, prepared by the Food and Agriculture Organization (FAO) [26], was used to establish the soil characteristics within the watershed.

- Metrological data

Satellite-derived precipitation data were downloaded from the Tropical Rainfall Measuring Mission (TRMM 3B42) [33], while temperature data were acquired from the Climate Prediction Center (CPC) [34].

- Hydrological data

Monthly streamflow data for 2005–2017 were acquired from the Central Water Commission (CWC) of India to support the SWAT model simulation.

### 2.2.2. Satellite Data Processing

Landsat images for the years 2005, 2011, and 2017 were preprocessed using Environment for Visualizing Images (ENVI) software version 4.8 to ensure high-quality data for analysis. Radiometric and atmospheric corrections were applied to address sensor calibration issues and atmospheric distortions, ensuring uniform reflectance values across the images. Additionally, the scan line corrector (SLC)-off failure in Landsat 7 ETM+ images was addressed using an advanced gap-filling technique within ENVI. Missing pixel values were reconstructed using spatial interpolation methods that leveraged the spectral properties of neighboring valid pixels, preserving spatial coherence. These corrections ensured that the reconstructed areas were consistent with the surrounding landscape and maintained the integrity of the spectral and spatial data. The geometrically corrected and gap-filled images were then imported into ArcGIS to generate accurate LULC maps for subsequent analysis. A supervised classification was subsequently conducted using the maximum likelihood algorithm, categorizing the photos into established LULC classes, including 'Deciduous Forest' (FRSD), 'Agriculture region' (AGRL), 'Urban Area' (URMD), 'Mixed Forest' (FRST), 'Range Land' (RNGE), 'Brush Land' (RNGB), 'Barren Land' (SWRN), 'Evergreen Forest' (FRSE), 'Pasture' (PAST), 'Water bodies' (WATR), and 'Orchard' (ORCD). Finally, an independent set of validation points was employed to verify the accuracy of the categorized output LULC maps. These validation points were systematically collected from high-resolution satellite imagery and ground-based datasets to ensure their reliability. The selection process aimed to achieve comprehensive spatial coverage across the study watersheds and to represent all major LULC classes. Additionally, the classification accuracy was evaluated using overall accuracy (OA) and kappa coefficient (KC) measures. The OA is the ratio of accurately categorized pixels to the total number of pixels (Equation (1)), while the KC accounts for chance agreement between observed and anticipated classifications (Equation (2)). Values of OA/KC approaching unity represent high accuracy/agreement [2].

$$OA = \frac{CP}{TP} \quad (1)$$

$$KC = \frac{X_{CC} - X_{CA}}{1 - X_{CA}} \quad (2)$$

where TP = total pixels; CP = correctly classified pixels;  $X_{CA}$  = a metric of the degree of agreement attributable to chance between the reference pixels and model predictions; and  $X_{CC}$  = the relative real correspondence among the categorized rasters.

### 2.2.3. SWAT Model Set Up

To calibrate and validate the SWAT model, critical input data were first imported, comprising the 2005 LULC map, a DEM, meteorological data, and a soil map, to delineate the watershed's spatial attributes and hydrological response units (HRUs). The DEM was utilized for watershed delineation, establishing the stream network and sub-basin borders. The soil and LULC data were subsequently integrated with the HRUs to model soil–water interactions and the impact of LULC on hydrological processes [35]. After all requisite data were entered, a sensitivity analysis was performed to determine the most significant parameters influencing streamflow. Parameters like the curve number (CN), soil accessible water content (AWC), and baseflow alpha factor (ALPHA\_BF) were analyzed to enhance model efficiency. Once the sensitive parameters had been identified, they were iteratively adjusted within the SWAT-CUP interface tool to align with observed data from 2005 for calibration and 2017 for validation, maximizing model outputs for streamflow [36]. The model calibration and validation were evaluated using the coefficient of determination ( $R^2$ ), Nash–Sutcliffe efficiency (NSE), and root mean square error. The calibrated and validated model is considered to exhibit high accuracy if  $R^2$  and NSE are over 0.5, the model efficiency increases as it approaches unity, and the model accuracy improves as RMSE approaches zero [37].

$$R^2 = \frac{\sum_{i=1}^{n^o} \left[ \left( Q_i^{\text{est}} - Q_{\text{avg}}^{\text{est}} \right) \left( Q_i^{\text{mea}} - Q_{\text{avg}}^{\text{mea}} \right) \right]^2}{\sum_{i=1}^{n^o} \left( Q_i^{\text{est}} - Q_{\text{avg}}^{\text{est}} \right)^2 \sum_{i=1}^{n^o} \left( Q_i^{\text{mea}} - Q_{\text{avg}}^{\text{mea}} \right)^2} \quad (3)$$

$$\text{NSE} = 1 - \frac{\sum_{i=1}^{n^o} \left( Q_i^{\text{mea}} - Q_i^{\text{est}} \right)^2}{\sum_{i=1}^{n^o} \left( Q_i^{\text{mea}} - Q_{\text{avg}}^{\text{mea}} \right)^2} \quad (4)$$

$$\text{RMSE} = \sqrt{\frac{1}{n^o} \sum_{i=1}^{n^o} \left( Q_i^{\text{mea}} - Q_i^{\text{est}} \right)^2} \quad (5)$$

where  $Q_i^{\text{est}}$ ,  $Q_i^{\text{mea}}$  = estimated and measured values of streamflow;  $Q_{\text{avg}}^{\text{est}}$ ,  $Q_{\text{avg}}^{\text{mea}}$  = mean value of the estimated and measured streamflow; and  $n^o$  = number of measurements.

### 2.2.4. Climate Change Scenarios

To assess the effects of climate change on hydrological systems, it is crucial to develop climate change scenarios that precisely depict future climatic circumstances [38]. These scenarios supply data for hydrological models and assist in forecasting future alterations in runoff and water availability. This research employed bias-corrected climate data obtained from downscaled global climate models (GCMs) to replicate two representative climate change scenarios (RCPs), i.e., RCP 4.5 (moderate) and RCP 8.5 (extreme), concentrating on projected alterations in temperature and precipitation [39].

- Bias correction of data

GCM data frequently exhibit intrinsic biases, including an overestimation of wet days and an underestimation of extreme precipitation events, which can impede their direct utilization in hydrological models. The delta change method was utilized for bias correction, substantially modifying climate estimates to better correspond with observed local data. This method utilized a change factor based on the ratio of mean future to mean historical values from GCM outputs, converting observed data into future projections while preserving local climate attributes. This ratio between forecast and historical precipitation

data adjusted for biases in rainfall frequency and intensity. The observed data were adjusted using the difference between estimated future and historical mean temperature values. This approach presumed that biases are both geographically unique and stable over time, enabling a dependable correction by correlating contemporary local discrepancies between observed and simulated values with future forecasts [40].

- Application of CMIP5 model

Future climate scenarios were produced with data from the CSIRO-Mk3.6.0 model within the CMIP5 suite, which were dynamically downscaled for regional accuracy by the CORDEX South Asia RegCM4 model. The Indian Institute of Tropical Meteorology (IITM) conducted the downscaling, enhancing spatial resolution to capture regional climate intricacies. The dynamically downscaled precipitation and temperature data were obtained from the Centre for Climate Change Research (CCCR) via the IITM website [41]. Two RCPs were chosen, namely, RCP 4.5, indicative of a moderate emissions scenario with stabilization by mid-century, and RCP 8.5, indicative of a high emissions scenario with substantial global warming effects. These pathways provide a thorough evaluation of possible hydrological alterations under moderate and extreme climatic conditions, aiding in the strategic planning of water resource management and climate adaptation [42].

#### 2.2.5. Development of Land Use/Land Cover Scenarios

The CA-Markov model was employed to generate future LULC scenarios for 2030 and 2040, functioning as an efficient tool for simulating spatial and temporal changes in LULC. The CA-Markov model integrates CA with Markov chain analysis, employing spatial dynamics and transition probabilities to predict changes in LULC over time [43]. In this study, LULC maps were utilized from 2005 and 2011 as inputs to train the algorithm, which was initially calibrated to predict the 2017 LULC map. The expected 2017 map was later validated against the actual 2017 map to ensure model precision, utilizing KC to assess categorization agreement. Crucial elements influencing alterations in LULC, such as proximity to roadways, water bodies, stream networks, DEM, and slope, were incorporated to address spatial dependency and enhance predictive precision [44].

The multi-layer perceptron (MLP) neural network was employed inside the CA-Markov framework to ascertain transition probabilities, effectively handling the complex, nonlinear relationships between driving forces and LULC transitions. The Markov chain component assessed transition probabilities among different LULC classes, while the CA element incorporated temporal and spatial interactions to depict genuine LULC changes. Following successful validation, the model was employed to simulate LULC scenarios for 2030 and 2040, providing insights into potential landscape changes under current trends and informing future planning and policy development [45].

#### 2.2.6. Running SWAT for Future Simulation of Runoff

Based on the preceding steps, the SWAT model was applied to predict runoff for the years 2030 and 2040, using the developed LULC and climate change scenarios as inputs. By incorporating these projections, SWAT can simulate hydrological processes across the watershed, capturing both temporal and spatial changes in runoff [46].

#### 2.2.7. Sustainability Implications

In this section, the primary challenges facing the watershed, driven largely by increased runoff, LULC changes, and climate change, are identified. Through an SAP, strategies aligned with SDGs to protect the watershed from further depletion are outlined, considering environmental, economic, and social perspectives, as reported elsewhere [47].

### 3. Results

#### 3.1. Accuracy Assessment of Land Use/Land Cover Classification

The evaluation of LULC maps across different watersheds demonstrated a noticeable improvement in classification accuracy over time, with all values approaching unity, signifying good reliability (Table 2). In the Wunna watershed, the OA increased from 84% in 2005 to 92% in 2017, while the KC increased from 0.82 to 0.88. In the Bharathapuzha watershed, OA rose from 85% in 2005 to 96% in 2017, while KC values improved from 0.83 to 0.89. In the Mahanadi watershed, the initial OA and KC values in 2005 were 91% and 0.88, respectively. Despite a slight variation in 2011, by 2017, the OA and KC had attained values of 96% and 0.89, respectively. The results, with all measures nearing unity, demonstrate the high classification accuracy and reliability of LULC maps across the three watersheds. The increasing accuracy of LULC maps established a solid basis for the SWAT model's hydrological simulations in the agro-climatic watersheds under investigation.

**Table 2.** Overall accuracy (OA), and Kappa coefficient (KC) during supervised classification for the following three Indian watersheds under investigation: Wunna, Bharathapuzha, and Mahanadi.

Watershed	Year	OA (%)	KC
Wunna	2005	84	0.82
	2011	87	0.81
	2017	92	0.88
Bharathapuzha	2005	85	0.83
	2011	88	0.85
	2017	96	0.89
Mahanadi	2005	91	0.88
	2011	87	0.84
	2017	96	0.89

Notes: OA = overall accuracy; and KC = Kappa coefficient.

#### 3.2. SWAT Calibration and Validation Output

A sensitivity analysis was conducted to identify the most influential input parameters for the SWAT model and ensure that the calibration process was finely tuned for optimal performance (see Supplementary Table S1). The subsequent accuracy assessment of the SWAT model across the three watersheds demonstrated a satisfactory predictive capability (Table 3). During the calibration phase,  $R^2$  values of 0.63, 0.60, and 0.81, NSE values of 0.63, 0.70, and 0.78, and RMSE values of 2.28, 1.18, and 1.89 were achieved for the Wunna, Bharathapuzha, and Mahanadi watersheds, respectively. These metrics indicate strong alignment with the observed streamflow data. The results from the validation phase further reinforced this reliability, with  $R^2$  values of 0.50, 0.62, and 0.75, NSE values of 0.51, 0.72, and 0.51, and RMSE values of 2.18, 2.17, and 2.17 for the respective watersheds. All  $R^2$  and NSE values exceeded the 0.5 threshold, and the RMSE values indicate acceptable error levels, confirming that the SWAT model was suitable and reliable for hydrological prediction across diverse agro-climatic conditions.



**Table 3.** Performance of SWAT model using calibration and validation phases for the following three Indian watersheds under investigation: Wunna, Bharathapuzha, and Mahanadi.

Watershed	Calibration Phase			Validation Phase		
	R <sup>2</sup>	NSE	RMSE	R <sup>2</sup>	NSE	RMSE
Wunna	0.63	0.63	2.28	0.50	0.51	2.18
Bharathapuzha	0.60	0.70	1.18	0.62	0.72	2.17
Mahanadi	0.81	0.78	1.89	0.75	0.51	2.17

Notes: R<sup>2</sup> = coefficient of determination; NSE = Nash–Sutcliffe efficiency; and RMSE = root mean square error.

### 3.3. Analysis of Climate Change Scenarios on Rainfall and Hydrological Patterns

The delta change approach for bias correction was employed to model future rainfall and wet day probabilities in the Bharathapuzha, Mahanadi, and Wunna watersheds under climate change scenarios, i.e., RCP 4.5 (moderate) and RCP 8.5 (extreme). Figure 3 depicts the likelihood of rainfall days based on long-term averages in the watersheds, whereas Figure 4 presents the distribution of yearly rainfall under historical, RCP 4.5, and RCP 8.5 scenarios.

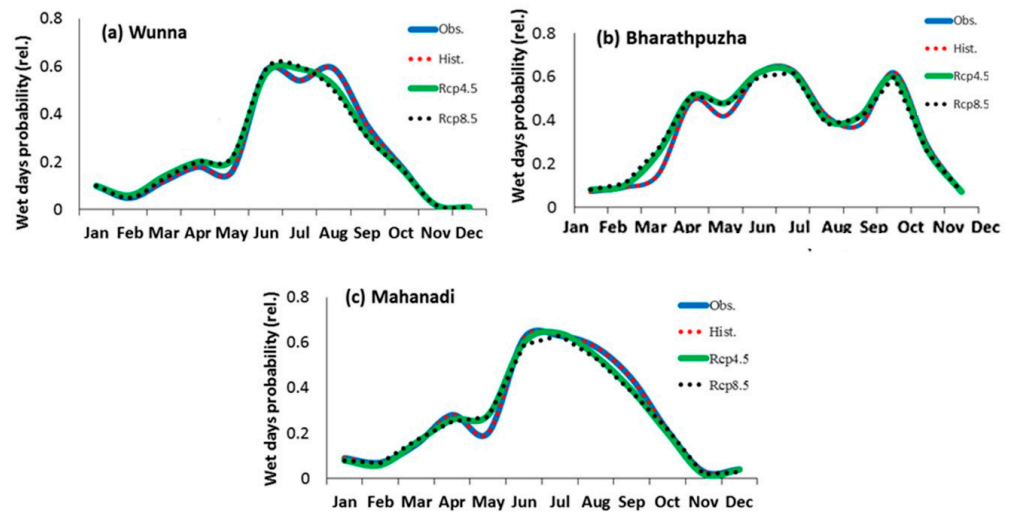


**Figure 3.** Probability of wet days for the Wunna, Bharathapuzha, and Mahanadi watersheds based on long-term averages: historical (2005–2017) and future scenarios (till 2030 and 2040) under RCP 4.5 and RCP 8.5.

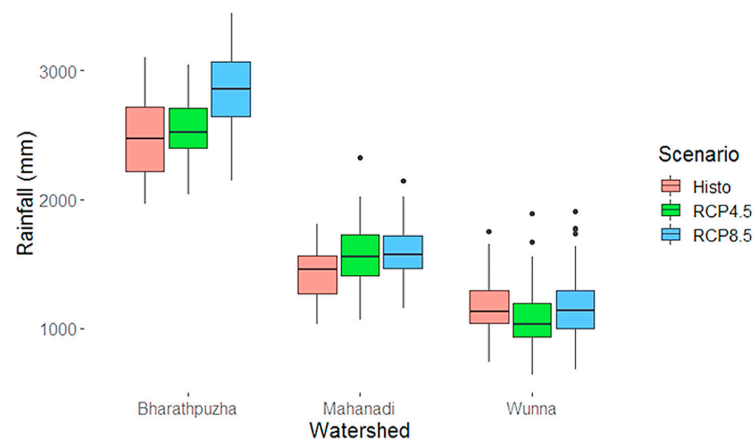


**Figure 4.** Box plot of historic and future annual rainfall (RCP 4.5 and 8.5 scenarios) for the following three Indian watersheds under investigation: Wunna, Bharathapuzha, and Mahanadi. The black circles represent outliers in the dataset.

Regarding the chance of rainy days (Figure 3), all three watersheds exhibited a distinct seasonal pattern, reaching a zenith during the monsoon months of June to September. The Wunna watershed (Figure 3a) had comparable probabilities for historical and prospective scenarios, with wet days reaching a peak of approximately 0.7, signifying stable frequency predictions for both RCP 4.5 and RCP 8.5. The Bharathapuzha watershed (Figure 3b) demonstrated a marginal rise in the chance of wet days under RCP 4.5 relative to historical data, with late monsoon probabilities approaching 0.75. The Mahanadi River (Figure 3c) adhered closely to historical trends, exhibiting a peak probability of approximately 0.65 for both future scenarios, indicating negligible alterations in wet day frequencies in these places according to climate forecasts.

The Bharathapuzha watershed exhibited the greatest susceptibility to climate change in terms of rainfall distribution (Figure 4). The historical median precipitation was approximately 2000 mm, but RCP 8.5 forecast a rise in extreme precipitation events, with the highest limit surpassing 3000 mm. The RCP 4.5 scenario exhibited a marginal reduction in median precipitation while maintaining a comparable range. Conversely, the median rainfall for the Mahanadi region consistently approximated 1000 mm across all scenarios, with a slight elevation in the upper range under RCP 8.5, signifying negligible alterations in rainfall distribution. The Wunna watershed also exhibited negligible alterations, with precipitation patterns in both RCP 4.5 and RCP 8.5 closely mirroring historical trends, indicating reduced susceptibility to prospective climate change scenarios.

The results in Figures 3 and 4 demonstrate that the rainfall responses differed among watersheds, although the RCP 4.5 and RCP 8.5 scenarios preserved the seasonal distribution of wet days. Bharathapuzha seemed increasingly susceptible to climate-induced surges in intense rainfall, especially under RCP 8.5, with possible ramifications for flood risk management. Conversely, the Mahanadi and Wunna watersheds exhibited enhanced stability in wet day probability and rainfall distribution, indicating that the hydrological effects of climate change may be less significant in these areas. This diversity highlights the need for customized watershed management techniques which consider the region's specific climate sensitivity.

### 3.4. Land Use/Land Cover Analysis

The CA-Markov model was employed to forecast LULC scenarios for 2030 and 2040 in the following three Indian watersheds under investigation: Wunna, Bharathapuzha, and Mahanadi. The spatial and temporal variations in actual LULC between 2005 and 2017 are depicted in Figure 5, while the predicted LULC changes from 2017 to 2040 are shown in Figure 6. The model was trained using the 2005 and 2011 LULC maps and validated using the 2017 LULC map, which demonstrated a perfect matching between the actual and predicted 2017 conditions. This high level of agreement underscored the reliability and accuracy of the CA-Markov model in simulating LULC dynamics and bolstered confidence in its ability to project future scenarios. The resultant LULC maps highlighted distinct trends, particularly the expansion of URMD and AGRL across the watersheds. Using a transition probability matrix (see Supplementary Table S2), the model revealed the likelihood of specific terrain types, such as RNGE, transitioning into URMD by 2040.

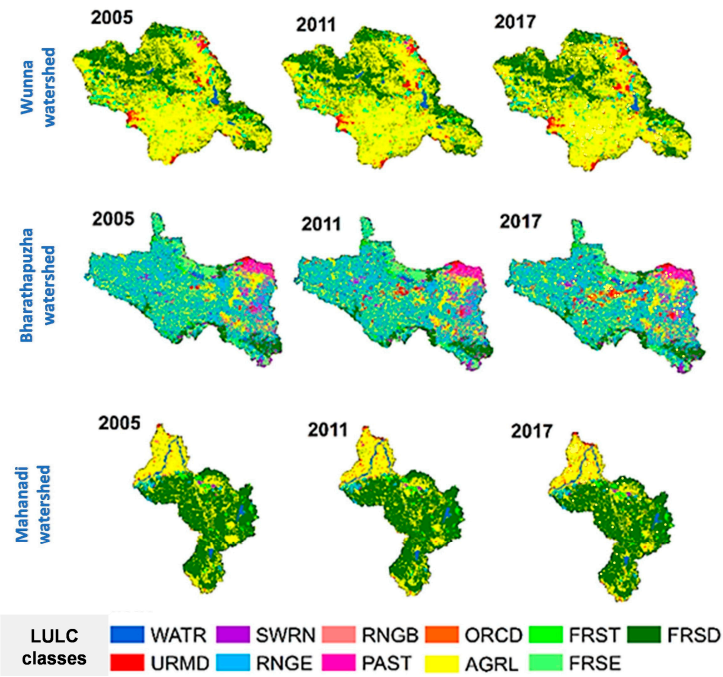


**Figure 5.** Spatial and temporal variations in actual land use/land cover (LULC) between 2005 and 2017 for the following three Indian watersheds under investigation: Wunna, Bharathapuzha, and Mahanadi. For LULC classes: FRSD = deciduous forest; AGRL = agricultural region; URMD = urban area; FRST = mixed forest; RNGE = range land; RNGB = brush land; SWRN = barren land; FRSE = evergreen forest; PAST = pasture; WATR = water bodies; and ORCD = orchard.

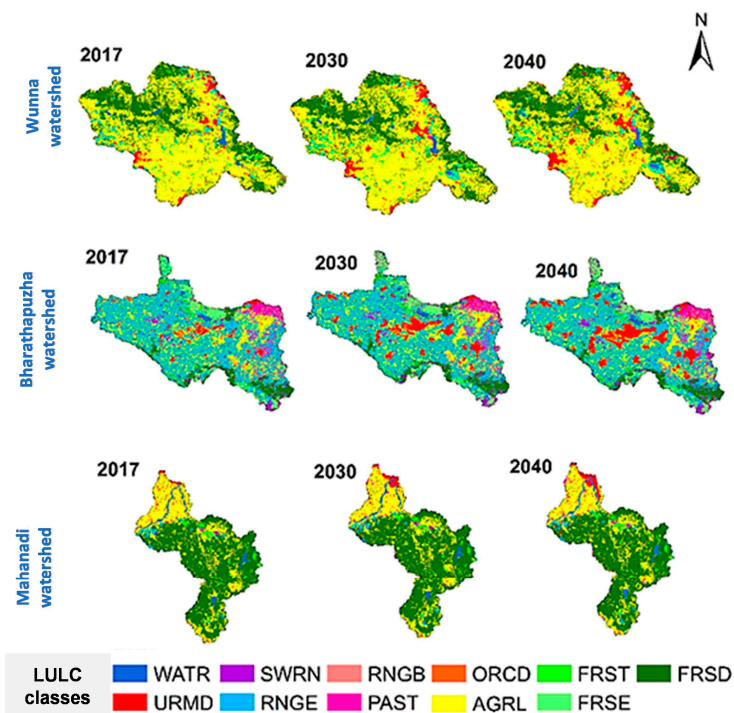


**Figure 6.** Spatial and temporal variations in predicted land use/land cover (LULC) between 2017 and 2040 for the following three Indian watersheds under investigation: Wunna, Bharathapuzha, and Mahanadi. For LULC classes: FRSD = deciduous forest; AGRL = agricultural region; URMD = urban area; FRST = mixed forest; RNGE = range land; RNGB = brush land; SWRN = barren land; FRSE = evergreen forest; PAST = pasture; WATR = water bodies; and ORCD = orchard.

The forecasts reveal a substantial tendency of URMD expansion across all three watersheds, with Bharathapuzha and Mahanadi undergoing the most significant alterations (Figure 5). In the Wunna watershed, URMD was projected to expand progressively, attaining 189.17 km<sup>2</sup> by 2030 and 222.27 km<sup>2</sup> by 2040, whilst AGRL was anticipated to diminish from 2908.25 km<sup>2</sup> in 2030 to 2862.12 km<sup>2</sup> by 2040. In addition to these changes, other LULC classes, e.g., FRSD, were anticipated to see conversions. The Bharathapuzha watershed was expected to witness URMD increase to 433.87 km<sup>2</sup> by 2030 and further expansion to 593.16 km<sup>2</sup> by 2040. AGRL was predicted to increase to 1514 km<sup>2</sup> by 2030 before experiencing a minor decline to 1457 km<sup>2</sup> by 2040. The extent of the WATR was projected to diminish from 90.37 km<sup>2</sup> in 2030 to 89.88 km<sup>2</sup> by 2040, accompanied by changes in other LULC groups. In the Mahanadi watershed, URMD was projected to expand consistently, growing to 113.63 km<sup>2</sup> by 2030 and 149.78 km<sup>2</sup> by 2040. AGRL was anticipated to grow steadily, reaching 1493.44 km<sup>2</sup> by 2030 and marginally declining to 1447.32 km<sup>2</sup> by 2040.

Table 4 listed the changes in the most significant LULC categories, i.e., URMD and AGRL, across the watersheds under investigation by 2030 and 2040. The Bharathapuzha watershed exhibited the most significant increase in URMD, which was anticipated to expand by 609% from 2005 to 2030, followed by an additional increase of 36.71% by 2040. This significant URMD expansion coincided with a 25.01% increase in AGRL by 2030, followed by a modest rise of 3.77% by 2040, reflecting a dual trend of urban and agricultural development that transformed the watershed's environment. In the Mahanadi watershed, URMD was anticipated to expand substantially, with 775% growth by 2030 and a further 31.81% by 2040, highlighting fast urbanization. AGRL in Mahanadi was projected to increase by 14% by 2030, followed by a reduction of 3% by 2040 due to URMD expansion. This transition indicated a growing conflict among LULC in Mahanadi, where URMD might progressively intrude upon AGRL. Conversely, the Wunna watershed underwent a more gradual transformation, with URMD anticipated to expand by 72.7% by 2030 and a further 17.39% by 2040. AGRL in Wunna was projected to shrink gradually, declining by -3.76% in 2030 and -1.58% in 2040, indicating a milder transition towards URMD relative to the other two watersheds. The percentage changes underscored differing pressures across the watersheds, highlighting the need for customized management measures to address the distinct dynamics of various LULC classes, especially URMD, in each region.

**Table 4.** Quantitative alteration in urban (URMD) and agriculture (AGRL) classes between 2005 and 2040 for the following three Indian watersheds under investigation: Wunna, Bharathapuzha, and Mahanadi.

Watershed	URMD Change (%)		AGRL Change (%)	
	2005–2030	2030–2040	2005–2030	2030–2040
Wunna	72.7	17.39	−3.76	−1.58
Bharathapuzha	609	36.71	25.01	3.77
Mahanadi	775	31.81	14	−3

Notes: URMD = urban area, and AGRL = agricultural region.

### 3.5. Future Variation in Runoff via SWAT

The SWAT model adopted climate change scenarios (RCP 4.5 and RCP 8.5), and LULC forecasts for 2030 and 2040 to predict future runoff in the three watersheds under investigation. This integrated methodology facilitated the analysis of both temporal and spatial patterns of surface runoff, as demonstrated in the following sections.

### 3.5.1. Temporal Variation Pattern

The mean temporal variation in surface runoff among the three watersheds exhibited unique patterns influenced by LULC and climatic conditions (Table 5). In the Wunna watershed, surface runoff exhibited modest increases, with measurements varying from 500.04 mm for RCP 4.5 in 2030 to 597.89 mm for RCP 8.5 in 2040. The forecasts indicated a 1.99% rise in runoff from 2030 LULC to 2040 LULC under RCP 4.5 and a 7.57% increase under RCP 8.5, suggesting that RCP 8.5 would yield greater runoff values. The Bharathapuzha watershed had escalating runoff trends, with RCP 8.5 forecasting values (1114.39 mm in 2030 and 1138 mm in 2040) higher than those forecast by RCP 4.5. For the Mahanadi, RCP 4.5 yielded greater surface runoff values than RCP 8.5, with runoff anticipated to decline marginally from 388.53 mm in 2030 to 375.76 mm in 2040 for RCP 8.5. The temporal study revealed that runoff was expected to be predominantly elevated in RCP 8.5 for Wunna and Bharathapuzha, whereas Mahanadi demonstrated a contrasting pattern, with greater values under RCP 4.5.

**Table 5.** Mean temporal variation in runoff by 2030 and 2040 for the following three Indian watersheds under investigation: Wunna, Bharathapuzha, and Mahanadi.

Watershed	LULC	Climate Scenario	Runoff (mm/yr)
Wunna	2030	RCP 4.5	500.04
		RCP 8.5	555.81
	2040	RCP 4.5	510.03
		RCP 8.5	597.89
Bharathapuzha	2030	RCP 4.5	834.22
		RCP 8.5	1114.39
	2040	RCP 4.5	853.38
		RCP 8.5	1138.00
Mahanadi	2030	RCP 4.5	388.53
		RCP 8.5	374.19
	2040	RCP 4.5	390.06
		RCP 8.5	375.76

Notes: LULC = land use/land cover, and RCP = representative concentration pathway.

### 3.5.2. Spatial Variation Pattern

High surface runoff was expected to spatially localize in particular areas within each watershed, indicating the cumulative consequences of swift URMD and climatic scenario influences (Figures 7–9). The Wunna watershed’s southeastern portion exhibited the highest runoff values, surpassing 600 mm for both RCP 4.5 and RCP 8.5 in 2030 and 2040, but the northwestern region displayed lower runoff values, remaining below 500 mm, particularly for RCP 4.5. The southern section of the Bharathapuzha watershed demonstrated the greatest runoff values, exceeding 1000 mm for both RCP 4.5 and RCP 8.5, which was attributed to increased URMD. In contrast, the northern region exhibited reduced runoff values, below 500 mm, especially for RCP 4.5. In the Mahanadi watershed, elevated runoff was predominantly observed in the northwestern area, exceeding 400 mm for both RCP scenarios, whereas the southern portion exhibited reduced flow, falling below 350 mm, especially for RCP 8.5. The spatial patterns revealed a persistent tendency toward elevated runoff values in areas undergoing substantial URMD expansion, particularly for the extreme RCP 8.5 scenario.



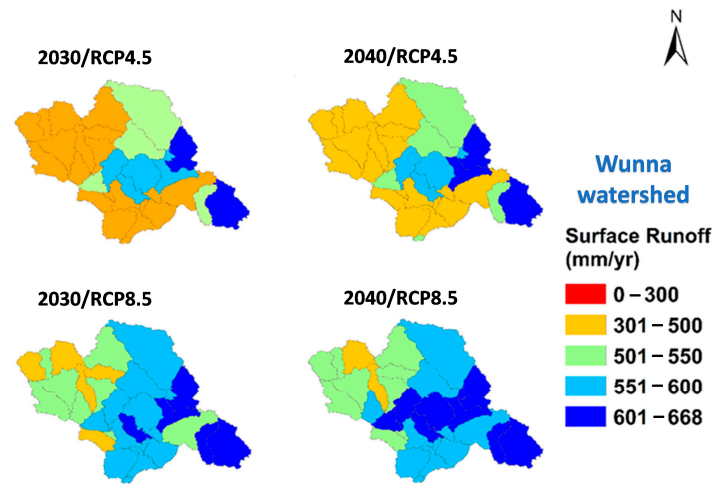


**Figure 7.** Distribution of predicted surface runoff for different scenarios of land use/land cover (LULC) in 2030/2040, and climate change (RCP 4.5/8.5) for Wunna watershed.

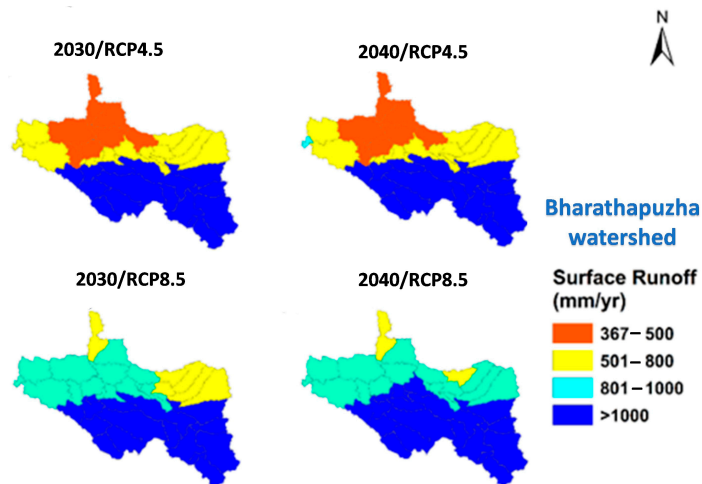


**Figure 8.** Distribution of predicted surface runoff for different scenarios of land use/land cover (LULC) in 2030/2040, and climate change (RCP 4.5/8.5) for Bharathapuzha watershed.

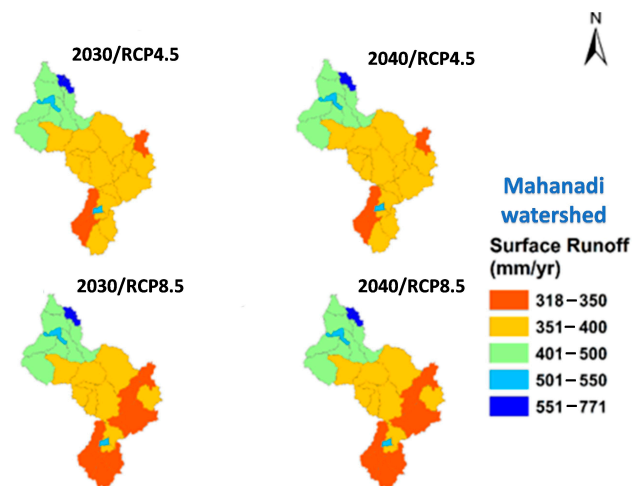


**Figure 9.** Distribution of predicted surface runoff for different scenarios of land use/land cover (LULC) in 2030/2040, and climate change (RCP 4.5/8.5) for Mahanadi watershed.

### 3.6. Sustainability Implications Associated with the Study Findings

#### 3.6.1. Emerging Challenges

The findings from the LULC and climate change scenarios in the Wunna, Bharathapuzha, and Mahanadi watersheds reveal considerable obstacles to attaining multiple SDGs (Figure 10). The predicted rise in surface runoff, propelled by accelerated URMD and heightened climate extremes (notably for RCP 8.5), presents immediate challenges to sustainable water management, climate resilience, and economic stability in these areas. Accelerated development may transform natural terrain, exacerbating surface runoff and flooding, especially in southeastern Wunna, southern Bharathapuzha, and northwestern Mahanadi. This unregulated URMD development reduces the soil’s natural absorption capacity, resulting in increased frequency and severity of flooding. Enhanced surface runoff accelerates soil erosion and diminishes water quality as contaminants from metropolitan regions flow into WATR, jeopardizing water resources. Moreover, the anticipated elevation in precipitation under RCP 8.5 may exacerbate these hydrological alterations and influence water resource management. In agricultural communities, economic stability is jeopardized when heightened runoff and soil erosion endanger crop yields and diminish soil productivity, compromising food security. Inequalities may be exacerbated if rural areas encounter limited access to clean water and resources as a result of runoff-induced pollution and flooding. Consequently, the results highlight the pressing need for an SAP to mitigate these environmental, economic, and social effects, guaranteeing that these watersheds can significantly contribute to the achievement of the SDGs.

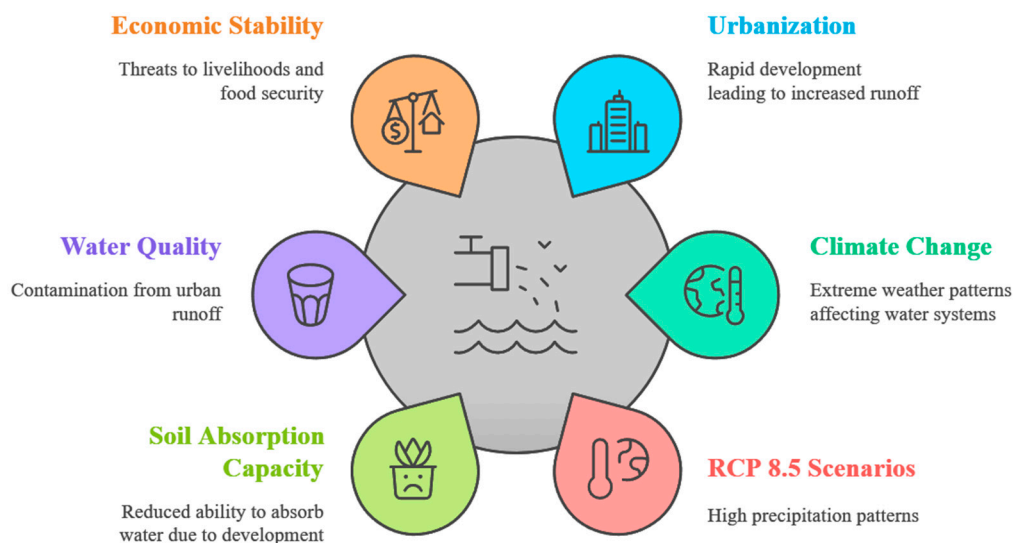


**Figure 10.** Challenges associated with the proposed scenarios of land use/land cover (LULC) and climate change for the following three Indian watersheds under investigation: Wunna, Bharathapuzha, and Mahanadi.

#### 3.6.2. Sustainable Action Plan (SAP)

An SAP is recommended to tackle the challenges of the anticipated rise in runoff and climate-related effects in the watersheds under investigation. The SAP is structured to match essential SDGs across environmental, economic, and social dimensions, guaranteeing that the proposed strategies advance SDGs while mitigating local vulnerabilities (Figure 11).

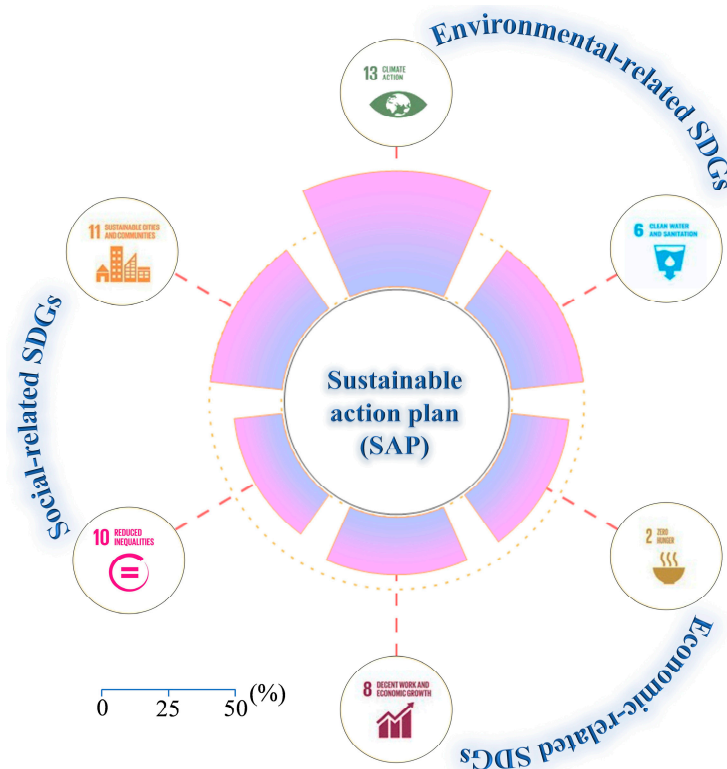


**Figure 11.** Quantitative contribution of the sustainable action plan (SAP) to the sustainability pillars across the following three Indian watersheds under investigation: Wunna, Bharathapuzha, and Mahanadi.

- Environment-related SDGs

**SDG 6. Clean Water and Sanitation:** The SAP addresses 25% (two out of eight) of SDG 6's targets, specifically enhancing water quality (Target 6.3) and safeguarding water-related ecosystems (Target 6.6). It emphasizes nature-based solutions, including wetland restoration, which filters contaminants from surface runoff, improving water quality before it enters into a bigger WATR. Riverbank stabilization and riparian buffer zones are essential components of the SAP to mitigate sedimentation and erosion, protect aquatic ecosystems, and preserve biodiversity within the watersheds. These measures directly tackle water pollution issues and address Target 6.3 by facilitating the natural filtration of contaminants, while riverbank stability (under Target 6.6) promotes long-term ecosystem health by mitigating the effects of excessive runoff.

**SDG 13. Climate Action:** The SAP addresses 40% (two out of five) of the targets of SDG 13, notably emphasizing the enhancement of resilience to climate impacts (Target 13.1) and the incorporation of climate measures into local planning (Target 13.2). It seeks to mitigate flood hazards and improve adaptation capability through climate-resilient infrastructure such as permeable pavements and green stormwater systems. Additionally, it guarantees that development aligns with long-term climate resilience objectives by integrating climate adaptation strategies into URMD design and agricultural practices. This strategy immediately addresses Target 13.1 by mitigating susceptibility to climate risks and fulfills Target 13.2 by integrating climate considerations into local LULC and resource management plans, promoting a proactive approach to climate-induced runoff escalation.

- Economic-related SDGs

**SDG 2. Zero Hunger:** The SAP contributes to 25% (two out of eight) of the targets of SDG 2 by promoting sustainable agriculture and raising productivity through methods that



address Target 2.3 (improving productivity and rural income) and Target 2.4 (advancing sustainable food production). It supports sustainable agriculture techniques, such as agro-forestry and no-till farming, to effectively reduce soil erosion and maintain soil production in the face of heightened runoff in AGR. Additionally, it enhances rural resilience to environmental stressors by offering resources and training in adaptive agricultural techniques to sustain farmers' incomes (Target 2.3) and promote soil conservation and sustainable yields (Target 2.4). These measures enhance food security and ensure long-term agricultural sustainability in the context of environmental changes.

**SDG 8. Decent Work and Economic Growth:** The SAP addresses 16.7% (two out of twelve) of SDG 8's targets. Specifically, it enhances economic resilience through resource efficiency (Target 8.4) and promotes infrastructure investment that cultivates resilient economies (Target 8.2). It also mitigates the environmental effects of URMD growth by advocating for resource-efficient URMD planning and facilitating sustainable infrastructure development. In addition, it promotes investment in water-efficient systems and infrastructure, enhancing the local economy's resilience to environmental variation and aligning with Target 8.2's focus on economic variety. These measures enhance resource use efficiency and tackle environmental issues, fostering sustainable development throughout the watersheds under investigation.

- **Social-related SDGs**

**SDG 10. Reduced Inequalities:** The SAP addresses 20% (two out of ten) of the targets of SDG 10 by emphasizing the promotion of social inclusion (Target 10.2) and the assurance of equal access to resources (Target 10.3). Moreover, it can empower vulnerable populations and promote inclusion in watershed management by emphasizing equitable access to clean water and engaging marginalized communities in decision-making. Furthermore, SAP's implementation of community-based water quality monitoring programs guarantees that resource access is equitable and balanced across various social groups. This direct involvement addresses Target 10.2 by facilitating the engagement of vulnerable populations and Target 10.3 by tackling sources of disparities and promoting the equitable distribution of water resources.

**SDG 11. Sustainable Cities and Communities:** The SAP contributes to 20% (two out of ten) of the targets of SDG 11 by improving URMD resilience through the reduction in catastrophe risk (Target 11.5) and minimizing environmental impact (Target 11.6). Also, it seeks to safeguard populations from runoff-induced flooding through flood control strategies and deliberate URMD planning, leading to a reduction in potential risks in susceptible URMD. Furthermore, the implementation of waste and runoff management systems by the SAP mitigates pollution and environmental degradation in metropolitan areas. These efforts correspond to Target 11.5's objective of mitigating disaster-related risks and Target 11.6's focus on decreasing per capita environmental impacts, fostering safer URMD settings within the watersheds under investigation.

#### **4. Discussion**

The previous research has established SWAT's efficacy in forecasting runoff under diverse LULC and climatic conditions, validating the model's applicability in areas experiencing swift URMD development and climatic oscillations [48]. Nevertheless, in the current study, a comprehensive evaluation was successfully provided of the runoff forecasts in the Wunna, Bharathapuzha, and Mahanadi watersheds by utilizing the SWAT model and incorporating climate change scenarios (RCP 4.5 and RCP 8.5) alongside future LULC estimates for 2030 and 2040. This study can be considered essential as it may offer a predictive understanding of hydrological alterations in various agro-climatic zones, facilitating watershed management planning, and solving any difficulties associated with water availability,

flood hazards, and soil erosion. These findings aligned with research using the water Gini coefficient, which can highlight disparities in water resource distribution due to uneven urban development and regional climatic variability [49].

The SWAT model was successfully calibrated and validated, employing high-precision LULC maps alongside meteorological data. The accuracy assessment revealed a high OA and KC, with values of 92% and 0.88, respectively, for the Wunna watershed, along with similarly elevated values for the Bharathapuzha and Mahanadi watersheds. These parameters were close to or beyond the performance documented in previous SWAT studies, where OA generally falls between 80% and 90% [50]. Moreover, model validation yielded acceptable  $R^2$ , NSE, and RMSE values across all watersheds (e.g., reaching 0.62, 0.72, and 2.17, respectively, in the Bharathapuzha watershed), which either coincide with or exceed the values reported in comparable studies [51]. The strong correlation between predicted and observed streamflow data highlighted SWAT's effectiveness in accurately predicting runoff, particularly when supported by dependable LULC and climate data. These findings were comparable to studies utilizing the Shannon index, which can evaluate environmental hazard distributions and confirm that areas with elevated runoff, like southern Bharathapuzha, are particularly vulnerable to hydrological extremes [52].

The incorporation of climate change scenarios (RCP 4.5 and RCP 8.5) demonstrated clear patterns in surface runoff, aligning with results from prior investigations utilizing SWAT under climate scenarios [53]. The study findings under the RCP 8.5 scenario illustrated a significant rise in surface runoff throughout all watersheds, reflecting patterns noted in previous global scenarios. Enhanced rainfall intensity and modified seasonal distributions under RCP 8.5 can exacerbate runoff, as reported elsewhere [54]. The current paper contributed to the existing literature by affirming that RCP 8.5 was likely to intensify hydrological extremes, particularly in areas experiencing URMD expansion. These results resonated with findings from studies employing the water Gini coefficient, which often highlighted how such climatic and urbanization-induced changes lead to uneven access to water resources, increasing challenges for equitable resource management [55].

The LULC predictions for 2030 and 2040 indicated significant URMD expansion, which impacts runoff by diminishing infiltration and augmenting surface flow. These results were consistent with those of international research indicating that URMD can be considered a primary factor contributing to increased runoff [56]. The Bharathapuzha watershed, anticipated to undergo substantial URMD expansion, exhibited the greatest rise in surface runoff, matching research conducted in rapidly urbanizing areas like the Loess Plateau in China [57]. This consistency indicated that SWAT can be adept at capturing the hydrological effects of LULC shifts, particularly when urbanization may be considered a significant factor [58]. Furthermore, findings from studies using the Shannon index confirmed that urban expansion in vulnerable areas often magnifies environmental hazards such as flooding and erosion, reinforcing the importance of sustainable urban planning [59].

The forecasts of heightened runoff in urban and rural areas were consistent with established patterns in hydrological studies, highlighting the cumulative effects of climate and LULC changes on runoff behavior [60]. High runoff concentrations, noted in the southeastern Wunna, southern Bharathapuzha, and northwestern Mahanadi regions demonstrated that URMD growth exacerbated runoff, particularly under RCP 8.5. Research in similar agro-climatic regions has reported elevated runoff rates in the context of URMD expansion, which was attributable to diminished infiltration and widespread impermeable surfaces [17]. Moreover, the elevation in sediment yield during heavy runoff conditions was consistent with the existing findings in the literature [61], as elevated runoff rates can exacerbate soil erosion, particularly in watersheds characterized by significant urban activity. These findings paralleled studies employing the Shannon index and water Gini

coefficient, which can highlight that urban and rural areas experience runoff and erosion impacts differently, further underscoring the need for equitable infrastructural planning to mitigate these disparities [62].

The results of this study highlighted significant obstacles in attaining many SDGs, especially SDG 6 (Clean Water and Sanitation) and SDG 13 (Climate Action). The anticipated increases in runoff under both climate and LULC scenarios could cause problems related to water resource management, particularly in flood-prone areas. The elevated runoff under RCP 8.5 may indicate a greater danger of floods, potentially undermining progress toward SDG 11 (Sustainable Cities and Communities) by jeopardizing urban infrastructure. The proposed SAP was consistent with SDG targets, tackling water quality (SDG 6) with green infrastructure that purifies pollutants and enhances infiltration [47]. The SAP can achieve climate resilience (SDG 13) by advocating for adaptive infrastructure, reflecting ideas from other watershed studies that can underscore the importance of proactive adaptation measures in water resource management [5]. These findings also can echo the outcomes of studies using the Shannon index to assess environmental hazards, emphasizing the role of targeted adaptation strategies to alleviate risks in vulnerable areas [63]. The study outcomes demonstrated that incorporating climate and LULC factors into SWAT applications can inform policies that may promote alignment with SDGs and aid in the mitigation of negative environmental, economic, and social effects [64,65].

## 5. Conclusions and Future Research

In this study, the SWAT model was applied to simulate and predict runoff across three distinct Indian watersheds, namely, Wunna, Bharathapuzha, and Mahanadi, under various LULC and climate change scenarios. The SWAT model integrated high-resolution satellite imagery, CA-Markov modeling for future LULC projections, and climate data under RCP 4.5 and RCP 8.5 conditions. The research demonstrated the model's efficacy by achieving reliable calibration and validation with  $R^2$  and NSE values greater than 0.50. The study findings revealed significant runoff >1000 mm by 2040 under the RCP 8.5 scenario in Bharathapuzha, particularly in the southern regions. Similarly, the southeastern Wunna watershed was expected to face heightened runoff exceeding 600 mm under RCP 8.5. The Mahanadi watershed, especially in the northwestern region, was anticipated to see runoff levels surpassing 400 mm. These elevated runoff estimates were the result of rapid urban expansion in the watersheds under investigation. The challenges associated with elevated runoff could threaten the targets of SDG 6 and 13, leading to potential water quality degradation and flood hazards. The SAP addressed these issues through nature-based solutions, such as wetland restoration and riverbank stabilization, contributing to 25% of SDG 6 targets, like improving water quality and protecting aquatic ecosystems, and 40% of SDG 13 targets by enhancing climate resilience. The SAP further promotes sustainable practices, matching other economic and social targets of SDGs.

While this study demonstrated the effectiveness of the SWAT model, it was limited to three agro-climatic zones, and the resolution of climate and satellite data may restrict fine-scale accuracy. Additionally, the accuracy of long-term projections, such as for 2030 and 2040, was constrained by the inherent uncertainties in predicting dynamic LULC and socio-economic changes over extended periods. Future research should expand the methodology to more regions, incorporate high-resolution datasets, and integrate advanced machine-learning techniques to enhance predictive performance. Including sediment data in SWAT calibration could also improve its ability to evaluate erosion dynamics, supporting more comprehensive and sustainable watershed management strategies. Furthermore, periodic re-evaluation of LULC projections using updated datasets could reduce uncertainties and ensure their reliability for long-term planning.

**Supplementary Materials:** The following supporting information can be downloaded at: <https://www.mdpi.com/article/10.3390/w17030458/s1>, Table S1. Results of sensitivity analysis during calibration of the SWAT model for three watersheds. Table S2. Transition probability matrix of land use/land cover (LULC) from 2011 to 2017.

**Author Contributions:** Conceptualization, S.S., N.A. and A.M.S.; data curation, L.S. and R.R.; formal analysis, Y.M.Y., D.D. and A.M.S.; funding acquisition, N.A.; investigation, R.R.; methodology, S.S., Y.M.Y., L.S., R.V. and A.M.S.; project administration, S.S. and N.A.; resources, N.A. and R.R.; software, S.S., R.V., and A.M.S.; supervision, Y.M.Y. and D.D.; validation, S.S. and L.S.; visualization, L.S., R.V. and A.M.S.; writing—original draft, S.S., L.S., R.R. and R.V.; writing—review and editing, Y.M.Y., D.D., N.A., R.V. and A.M.S. All authors have read and agreed to the published version of the manuscript.

**Funding:** This research received no external funding.

**Data Availability Statement:** The original contributions presented in this study are included in the article/Supplementary Materials; further inquiries can be directed to the corresponding author.

**Acknowledgments:** This research was supported by the Researchers Supporting Project number (RSPD2025R804), King Saud University, Riyadh, Saudi Arabia.

**Conflicts of Interest:** The authors declare no conflicts of interest.

## References

- Govender, T.; Dube, T.; Shoko, C. Remote sensing of land use-land cover change and climate variability on hydrological processes in Sub-Saharan Africa: Key scientific strides and challenges. *Geocarto Int.* **2022**, *37*, 10925–10949. [[CrossRef](#)]
- Saqr, A.M.; Nasr, M.; Fujii, M.; Yoshimura, C.; Ibrahim, M.G. Monitoring of Agricultural Expansion Using Hybrid Classification Method in Southwestern Fringes of Wadi El-Natron, Egypt: An Appraisal for Sustainable Development. In Proceedings of the ACESD 2022: Asia Conference on Environment and Sustainable Development, Kyoto, Japan, 4–6 November 2022; Springer Nature: Singapore, 2023; pp. 349–362. [[CrossRef](#)]
- Stephens, C.M.; Lall, U.; Johnson, F.M.; Marshall, L.A. Landscape changes and their hydrologic effects: Interactions and feedbacks across scales. *Earth-Sci. Rev.* **2021**, *212*, 103466. [[CrossRef](#)]
- Noman, M.; Ullah, I.; Khan, M.A.; Qazi, A.; Farooq, W.; Saqr, A.; Elsheikh, A. Analysis of overcurrent protective relaying as minimum adopted fault protection for small-scale hydropower plants. *Int. J. Environ. Sci. Technol.* **2024**, *21*, 4457–4470. [[CrossRef](#)]
- Paudel, G.; Pant, R.R.; Joshi, T.R.; Saqr, A.M.; Durin, B.; Cetl, V.; Kamble, P.N.; Bishwakarma, K. Hydrochemical Dynamics and Water Quality Assessment of the Ramsar-Listed Ghodaghodi Lake Complex: Unveiling the Water-Environment Nexus. *Water* **2024**, *16*, 3373. [[CrossRef](#)]
- Barbhuiya, S.; Manekar, A.; Ramadas, M. Performance evaluation of ML techniques in hydrologic studies: Comparing streamflow simulated by SWAT, GR4J, and state-of-the-art ML-based models. *J. Earth Syst. Sci.* **2024**, *133*, 3. [[CrossRef](#)]
- Gao, S.; Zhang, S.; Huang, Y.; Han, J.; Zhang, T.; Wang, G. A hydrological process-based neural network model for hourly runoff forecasting. *Environ. Model. Softw.* **2024**, *176*, 106029. [[CrossRef](#)]
- Ji, C.; Cao, Y.; Li, X.; Pei, X.; Sun, B.; Yang, X.; Zhou, W. A review of the satellite remote sensing techniques for assessment of runoff and sediment in soil erosion. *J. Hydrol. Hydromech.* **2024**, *72*, 252–267. [[CrossRef](#)]
- Mensah, J.K.; Ofose, E.A.; Yidana, S.M.; Akpoti, K.; Kabo-bah, A.T. Integrated modeling of hydrological processes and groundwater recharge based on land use land cover, and climate changes: A systematic review. *Environ. Adv.* **2022**, *8*, 100224. [[CrossRef](#)]
- Francesconi, W.; Srinivasan, R.; Pérez-Miñana, E.; Willcock, S.P.; Quintero, M. Using the Soil and Water Assessment Tool (SWAT) to model ecosystem services: A systematic review. *J. Hydrol.* **2016**, *535*, 625–636. [[CrossRef](#)]
- Kiprotich, P.; Wei, X.; Zhang, Z.; Ngigi, T.; Qiu, F.; Wang, L. Assessing the impact of land use and climate change on surface runoff response using gridded observations and swat+. *Hydrology* **2021**, *8*, 48. [[CrossRef](#)]
- Aloui, S.; Mazzoni, A.; Elomri, A.; Aouissi, J.; Boufekane, A.; Zghibi, A. A review of Soil and Water Assessment Tool (SWAT) studies of Mediterranean catchments: Applications, feasibility, and future directions. *J. Environ. Manag.* **2023**, *326*, 116799. [[CrossRef](#)] [[PubMed](#)]
- Mohseni, U.; Agnihotri, P.G.; Pande, C.B.; Durin, B. Understanding the Climate Change and Land Use Impact on Streamflow in the Present and Future under CMIP6 Climate Scenarios for the Parvara Mula Basin, India. *Water* **2023**, *15*, 1753. [[CrossRef](#)]
- Cao, C.; Sun, R.; Wu, Z.; Chen, B.; Yang, C.; Li, Q.; Fraedrich, K. Streamflow Response to Climate and Land-Use Changes in a Tropical Island Basin. *Sustainability* **2023**, *15*, 13941. [[CrossRef](#)]
- Zhao, J.; Zhang, N.; Liu, Z.; Zhang, Q.; Shang, C. SWAT model applications: From hydrological processes to ecosystem services. *Sci. Total Environ.* **2024**, *931*, 172605. [[CrossRef](#)] [[PubMed](#)]



16. Lucas-Borja, M.E.; Carrà, B.G.; Nunes, J.P.; Bernard-Jannin, L.; Zema, D.A.; Zimbone, S.M. Impacts of land-use and climate changes on surface runoff in a tropical forest watershed (Brazil). *Hydrol. Sci. J.* **2020**, *65*, 1956–1973. [[CrossRef](#)]
17. Haseeb, F.; Ali, S.; Ahmed, N.; Alarifi, N.; Youssef, Y.M. Comprehensive Probabilistic Analysis and Practical Implications of Rainfall Distribution in Pakistan. *Atmosphere* **2025**, *16*, 122. [[CrossRef](#)]
18. Bolan, S.; Padhye, L.P.; Jasemizad, T.; Govarthanam, M.; Karmegam, N.; Wijesekara, H.; Amarasiri, D.; Hou, D.; Zhou, P.; Biswal, B.K.; et al. Impacts of climate change on the fate of contaminants through extreme weather events. *Sci. Total Environ.* **2024**, *909*, 168388. [[CrossRef](#)] [[PubMed](#)]
19. Matthan, T. Beyond bad weather: Climates of uncertainty in rural India. *J. Peasant. Stud.* **2023**, *50*, 114–135. [[CrossRef](#)]
20. Pankaj, P.K.; Gaur, M.K.; Nirmala, G.; Maruthi, V.; Pushpanjali; Samuel, J.; Reddy, K.S. Diversification and land use management practices for food and nutritional security under the climate change scenario in arid and semi-arid regions of India. In *Food Security and Land Use Change under Conditions of Climatic Variability: A Multidimensional Perspective*; Springer: Berlin/Heidelberg, Germany, 2020; pp. 281–309. [[CrossRef](#)]
21. Raunaq; Kumar, L.S.; Arya, S.V.; Singh, S.B. Adsorption-desorption of tebuconazole in three soils. *Pestic. Res. J.* **2017**, *29*, 82–87.
22. Patra, S.; Shilky; Kumar, A.; Saikia, P. Impact of Land Use Systems and Climate Change on Water Resources: Indian Perspectives. In *Advances in Water Resource Planning and Sustainability*; Springer Nature: Singapore, 2023; pp. 97–110. [[CrossRef](#)]
23. CWC. NRSC Godavari Basin Report. Minist. Water Resour. Version 2 2014. Available online: [www.india-wris.nrsc.gov.in](http://www.india-wris.nrsc.gov.in) (accessed on 15 December 2024).
24. CWC. NRSC West Flowing Rivers from Tadri to Kanyakumari. Minist. Water Resour. Version 2 2014, 1–150. Available online: [www.india-wris.nrsc.gov.in](http://www.india-wris.nrsc.gov.in) (accessed on 15 December 2024).
25. Singh, L.; Saravanan, S. Satellite-derived GRACE groundwater storage variation in complex aquifer system in India. *Sustain. Water Resour. Manag.* **2020**, *6*, 3. [[CrossRef](#)]
26. Banela, M.; Kyvelou, S.S.; Kitsiou, D. Mapping and Assessing Cultural Ecosystem Services to Inform Maritime Spatial Planning: A Systematic Review. *Heritage* **2024**, *7*, 697–736. [[CrossRef](#)]
27. Rasheed, N.J.; Al-Khafaji, M.S.; Alwan, I.A.; Al-Suwaiyan, M.S.; Doost, Z.H.; Yaseen, Z.M. Survey on the resolution and accuracy of input data validity for SWAT-based hydrological models. *Heliyon* **2024**, *10*, e38348. [[CrossRef](#)] [[PubMed](#)]
28. Samsudin, M.S.; Azid, A.; Zaudi, M.A.; Adam, M.R.; Sani, M.S.A.; Saharuddin, S.M.; Ibrahim, A.; Nasir, M.F.M.; Tan, M.L.; Ali, N.I.M. Analyzing Agricultural Land Use with Cellular Automata-MARCOV and Forecasting Future Marine Water Quality Index: A Case Study in East Coast Peninsular Malaysia. *Water. Air. Soil Pollut.* **2024**, *235*, 8. [[CrossRef](#)]
29. Prabhjyot-Kaur; Sandhu, S.S.; Kothiyal, S. Optimising Sowing Window for Wheat Cultivars Under RCP 4.5 and RCP 6.0 Scenarios During the 21st Century in Indian Punjab. *J. Agron. Crop Sci.* **2024**, *210*, e12711. [[CrossRef](#)]
30. Ren, C.; Deng, X.; Zhang, H.; Yu, L. Assessing the Hydrological Response to Land Use Changes Linking SWAT and CA-Markov Models. *Hydrol. Process.* **2024**, *38*, e15341. [[CrossRef](#)]
31. USGS Homepage. Available online: <https://earthexplorer.usgs.gov/> (accessed on 15 December 2024).
32. Available online: <https://search.earthdata.nasa.gov/search> (accessed on 15 December 2024).
33. Huffman, G.J.; Adler, R.F.; Bolvin, D.T.; Gu, G.; Nelkin, E.J.; Bowman, K.P.; Hong, Y.; Stocker, E.F.; Wolff, D.B. The TRMM Multisatellite Precipitation Analysis (TMPA): Quasi-global, multiyear, combined-sensor precipitation estimates at fine scales. *J. Hydrometeorol.* **2007**, *8*, 38–55. [[CrossRef](#)]
34. Chen, M.; Shi, W.; Xie, P.; Silva, V.B.S.; Kousky, V.E.; Higgins, R.W.; Janowiak, J.E. Assessing objective techniques for gauge-based analyses of global daily precipitation. *J. Geophys. Res. Atmos.* **2008**, *113*, 4. [[CrossRef](#)]
35. Masria, A.; Nadaoka, K.; Negm, A.; Iskander, M. Detection of shoreline and land cover changes around Rosetta Promontory, Egypt, based on remote sensing analysis. *Land* **2015**, *4*, 216–230. [[CrossRef](#)]
36. Maitso, O. Effects of Land-Use/Land Cover Changes on Flow and Sedimentation from the Metsimotlhabe River Catchment Using Soil and Water Assessment Tool (SWAT) Model. Doctoral Dissertation, Botswana University of Agriculture and Natural Resources, Gaborone, Botswana, 2020.
37. Saqr, A.M.; Nasr, M.; Fujii, M.; Yoshimura, C.; Ibrahim, M.G. Optimal Solution for Increasing Groundwater Pumping by Integrating MODFLOW-USG and Particle Swarm Optimization Algorithm: A Case Study of Wadi El-Natron, Egypt. In Proceedings of the 2022 12th International Conference on Environment Science and Engineering, Beijing, China, 2–5 September 2022; ICESE 2022. Springer: Singapore, 2023; pp. 59–73. [[CrossRef](#)]
38. Alao, J.O.; Ayejoto, D.A.; Fahad, A.; Mohammed, M.A.A.; Saqr, A.M.; Joy, A.O. Environmental Burden of Waste Generation and Management in Nigeria. In *Technical Landfills and Waste Management: Volume 2: Municipal Solid Waste Management*; Springer Nature: Cham, Switzerland, 2024; pp. 27–56. [[CrossRef](#)]
39. Hasan, M.A.; Islam, A.K.M.S.; Akanda, A.S. Climate projections and extremes in dynamically downscaled CMIP5 model outputs over the Bengal delta: A quartile based bias-correction approach with new gridded data. *Clim. Dyn.* **2018**, *51*, 2169–2190. [[CrossRef](#)]

40. Maraun, D.; Widmann, M. Statistical Downscaling and Bias Correction for Climate Research. In *Statistical Downscaling and Bias Correction for Climate Research*; Cambridge University Press: Cambridge, UK, 2018. [[CrossRef](#)]
41. Sanjay, J.; Ramarao, M.V.S.; Mahesh, R.; Ingle, S.; Singh, B.B.; Krishnan, R. Regional Climate Change Datasets for South Asia. *arXiv* **2020**, arXiv:2012.10387.
42. Tan, G.; Ayugi, B.; Ngoma, H.; Ongoma, V. Projections of future meteorological drought events under representative concentration pathways (RCPs) of CMIP5 over Kenya, East Africa. *Atmos. Res.* **2020**, *246*, 105112. [[CrossRef](#)]
43. Eastman, J.R.; Toledano, J. A short presentation of CA\_MARKOV. In *Geomatic Approaches for Modeling Land Change Scenarios*; Lecture Notes in Geoinformation and Cartography; Camacho Olmedo, M., Paegelow, M., Mas, J.F., Escobar, F., Eds.; Springer: Cham, Switzerland, 2018. [[CrossRef](#)]
44. Kuglerová, L.; Kielstra, B.W.; Moore, R.D.; Richardson, J.S. Importance of scale, land-use, and stream network properties for riparian plant communities along an urban gradient. *Freshw. Biol.* **2019**, *64*, 587–600. [[CrossRef](#)]
45. Aftab, B.; Wang, Z.; Wang, S.; Feng, Z. Application of a Multi-Layer Perceptron and Markov Chain Analysis-Based Hybrid Approach for Predicting and Monitoring LULCC Patterns Using Random Forest Classification in Jhelum District, Punjab, Pakistan. *Sensors* **2024**, *24*, 5648. [[CrossRef](#)] [[PubMed](#)]
46. Zhang, H.; Wang, B.; Liu, D.L.; Zhang, M.; Leslie, L.M.; Yu, Q. Using an improved SWAT model to simulate hydrological responses to land use change: A case study of a catchment in tropical Australia. *J. Hydrol.* **2020**, *585*, 124822. [[CrossRef](#)]
47. Timalisina, R.; Acharya, S.; Durin, B.; Awasthi, M.P.; Pant, R.R.; Joshi, G.R.; Byanju, R.M.; Panthi, K.P.; Joshi, S.; Kumar, A.; et al. An Assessment of Seasonal Water Quality in Phewa Lake, Nepal, by Integrating Geochemical Indices and Statistical Techniques: A Sustainable Approach. *Water* **2025**, *17*, 238. [[CrossRef](#)]
48. Abbaszadeh, M.; Bazrafshan, O.; Mahdavi, R.; Sardooi, E.R.; Jamshidi, S. Modeling Future Hydrological Characteristics Based on Land Use/Land Cover and Climate Changes Using the SWAT Model. *Water Resour. Manag.* **2023**, *37*, 4177–4194. [[CrossRef](#)]
49. Babuna, P.; Yang, X.; Tulcan, R.X.S.; Dehui, B.; Takase, M.; Guba, B.Y.; Han, C.; Awudi, D.A.; Li, M. Modeling water inequality and water security: The role of water governance. *J. Environ. Manag.* **2023**, *326*, 116815. [[CrossRef](#)] [[PubMed](#)]
50. Wang, S.; He, S.; Wang, J.; Li, J.; Zhong, X.; Cole, J.; Kurbanov, E.; Sha, J. Analysis of Land Use/Cover Changes and Driving Forces in a Typical Subtropical Region of South Africa. *Remote Sens.* **2023**, *15*, 4823. [[CrossRef](#)]
51. Michael Mamo, K.H.; Jain, M.K. Runoff and Sediment Modeling Using SWAT in Gumera Catchment, Ethiopia. *Open J. Mod. Hydrol.* **2013**, *03*, 196–205. [[CrossRef](#)]
52. Yang, W.; Xu, K.; Lian, J.; Ma, C.; Bin, L. Integrated flood vulnerability assessment approach based on TOPSIS and Shannon entropy methods. *Ecol. Indic.* **2018**, *89*, 269–280. [[CrossRef](#)]
53. Atmaja, T.; Setiawati, M.D.; Kurisu, K.; Fukushi, K. Advancing Coastal Flood Risk Prediction Utilizing a GeoAI Approach by Considering Mangroves as an Eco-DRR Strategy. *Hydrology* **2024**, *11*, 198. [[CrossRef](#)]
54. Xu, Z.; Ma, K.; Yuan, X.; He, D. Hydrologic Response to Future Climate Change in the Dulong-Irrawaddy River Basin Based on Coupled Model Intercomparison Project 6. *Chinese Geogr. Sci.* **2024**, *34*, 294–310. [[CrossRef](#)]
55. Yuan, Y.; Li, X.; Wang, H.; Geng, X.; Gu, J.; Fan, Z.; Wang, X.; Liao, C. Unraveling the global economic and mortality effects of rising urban heat island intensity. *Sustain. Cities Soc.* **2024**, *116*, 105902. [[CrossRef](#)]
56. Naik, M.; Abiodun, B.J. Modelling the potential of land use change to mitigate the impacts of climate change on future drought in the Western Cape, South Africa. *Theor. Appl. Climatol.* **2024**, *155*, 6371–6392. [[CrossRef](#)]
57. Zhao, H.; He, H.; Wang, J.; Bai, C.; Zhang, C. Vegetation restoration and its environmental effects on the Loess Plateau. *Sustainability* **2018**, *10*, 4676. [[CrossRef](#)]
58. Dolgorsuren, S.E.; Ishgaldan, B.; Myagmartseren, P.; Kumar, P.; Meraj, G.; Singh, S.K.; Kanga, S.; Almazroui, M. Hydrological Responses to Climate Change and Land-Use Dynamics in Central Asia's Semi-arid Regions: An SWAT Model Analysis of the Tuul River Basin. *Earth Syst. Environ.* **2024**, *8*, 297–323. [[CrossRef](#)]
59. Guan, Y.; Liu, J.; Cui, W.; Chen, D.; Zhang, J.; Lu, H.; Maeda, E.E.; Zeng, Z.; Beck, H.E. Elevation Regulates the Response of Climate Heterogeneity to Climate Change. *Geophys. Res. Lett.* **2024**, *51*, 483. [[CrossRef](#)]
60. Ho, M.; Nathan, R.; Wasko, C.; Vogel, E.; Sharma, A. Projecting changes in flood event runoff coefficients under climate change. *J. Hydrol.* **2022**, *615*, 128689. [[CrossRef](#)]
61. Rajasekar, A.; Murava, R.T.; Norgbey, E.; Zhu, X. Spatial Distribution, Risk Index, and Correlation of Heavy Metals in the Chuhe River (Yangtze Tributary): Preliminary Research Analysis of Surface Water and Sediment Contamination. *Appl. Sci.* **2024**, *14*, 904. [[CrossRef](#)]
62. Panda, D.; Pandit, R.S.; Sahu, B.; Kamaraju, R.; Barik, T.K. Understanding Mosquito Faunal Diversity: An Approach to Assess the Burden of Vector-Borne Diseases in Three Representative Topographies (Rural, Urban, and Peri-Urban) of Ganjam District in Odisha State, India. *J. Trop. Med.* **2024**, *2024*, 9701356. [[CrossRef](#)] [[PubMed](#)]
63. Chen, J.; Yin, S.; Yang, X. The impact of adaptive management on community resilience in arid rural areas facing environmental change: An integrated analytical framework. *Environ. Sci. Policy* **2023**, *150*, 103589. [[CrossRef](#)]

64. Sathiyamurthi, S.; Youssef, Y.M.; Gobi, R.; Ravi, A.; Alarifi, N.; Sivasakthi, M.; Kumar, S.P.; Dąbrowska, D.; Saqr, A.M. Optimal Land Selection for Agricultural Purposes Using Hybrid Geographic Information System–Fuzzy Analytic Hierarchy Process–Geostatistical Approach in Attur Taluk, India: Synergies and Trade-Offs Among Sustainable Development Goals. *Sustainability* **2025**, *17*, 809. [[CrossRef](#)]
65. Visweshwaran, R.; Ramsankaran, R.; Eldho, T.I.; Jha, M.K. Hydrological Impact Assessment of Future Climate Change on a Complex River Basin of Western Ghats, India. *Water* **2022**, *14*, 3571. [[CrossRef](#)]

**Disclaimer/Publisher’s Note:** The statements, opinions and data contained in all publications are solely those of the individual author(s) and contributor(s) and not of MDPI and/or the editor(s). MDPI and/or the editor(s) disclaim responsibility for any injury to people or property resulting from any ideas, methods, instructions or products referred to in the content.